

Behaviour of the Cr(III)/Cr(II) reaction on gold–graphite electrodes. Application to redox flow storage cell

M. Lopez-Atalaya, G. Codina, J. R. Perez, J. L. Vazquez* and A. Aldaz

Departamento de Química-Física, Universidad de Alicante, Apartado 99, 03080 Alicante (Spain)

M. A. Climent

Departamento de Ingeniería de la Construcción, Universidad Politécnica de Valencia, Apartado 328, 03080 Alicante (Spain)

(Received October 5, 1990)

Abstract

With the aim of increasing the efficiency of an Fe/Cr redox flow battery, the behaviour of the Cr(III)/Cr(II) redox reactions and the hydrogen evolution on gold–graphite electrodes has been studied. Different metals with high hydrogen overvoltage have been used. An enhancement in the reversibility of the redox couple is produced with these types of gold–graphite electrodes, though the energetic efficiency of a monopolar Fe/Cr redox cell constructed with these electrodes is not improved due to the greater hydrogen evolution presented by the gold–graphite electrodes in relation with graphite electrodes.

Introduction

A redox flow cell is an electrochemical device for bulk energy storage based on the use of two soluble redox couples separated by a highly selective ion exchange membrane.

Since the redox flow cell concept was first proposed by Thaller in 1974 [1], different redox couples have been investigated [2, 3]. More recently, an Fe(II)/Fe(III)//Cr(III)/Cr(II) aqueous cell using a chloride electrolyte has been developed at the NASA-Lewis Research Center [4, 5], the Ministry of International Trade and Industry of Japan [6], Siemens A-G, Erlangen, F.R.G. [7] and the University of Alicante, Spain [8, 9].

While the Fe(III)/Fe(II) couple exhibits a very high reversibility on carbonaceous electrodes (graphite and carbon) the kinetics of the Cr(III)/Cr(II) redox couple is very slow on these materials. Moreover, the hydrogen reduction process is a competitive reaction with the Cr(III) reduction ($E^\circ = -0.41$ versus NHE). So during recent years considerable efforts have been devoted to developing corrosion resistant materials which exhibit both good electrocatalytic activity for the chromium(III)/chromium(II) reaction

*Author to whom correspondence should be addressed.

and a high hydrogen overvoltage in order to improve the voltage and coulombic efficiencies of the iron/chromium redox flow cell.

Due to its high resistance to corrosion in HCl medium, graphite was chosen as the electrode material. However, its hydrogen overvoltage is not high enough to avoid hydrogen evolution and the chromium redox reaction rate on this material is too slow. Therefore, a catalyst would be desirable for the chromium couple in order to: (i) increase the rate and the reversibility of the redox reaction and (ii) decrease the rate of hydrogen evolution during the process of the charge of the battery because this evolution diminishes the coulombic efficiency and unbalances the posilite, Fe(III)/Fe(II) and negalite Cr(III)/Cr(II) electrolytes.

The electrochemical behaviour of the Cr(III)/Cr(II) couple on different electrodes in the presence of Pb(II) and Bi(III) ions has been studied by different authors [4, 5, 10–13]. The deposition of these metals on the electrode surface in HCl solutions not only enhances the rate of the Cr(III)/Cr(II) reaction but also increases the hydrogen overvoltage.

It is also known that gold is a good electrocatalyst for the Cr(III)/Cr(II) reaction [14] and that for gold–graphite electrodes either too little ($< 5 \mu\text{g}/\text{cm}^2$), or too great ($< 60 \mu\text{g}/\text{cm}^2$), an amount of gold produces a low electrocatalytic effect [10].

For this reason this study deals mainly with the electrocatalytic influence of lead and bismuth, either electrochemically deposited on gold–graphite electrodes or codeposited with gold on graphite electrodes, on the kinetics of the Cr(III)/Cr(II) reaction, and with the study of the behaviour of these electrodes in an Fe/Cr redox flow cell.

Experimental

The electrocatalytic properties of each electrode were studied using cyclic voltammetry. The electronic set-up comprised an HQ potentiostat, a PAR programmable sweep generator and an XY recorder.

A graphite working electrode, JP 845 (Le Carbon Lorraine) with a geometric surface area of 1 cm^2 was used. The surface of the electrode was polished with a 600 grit silicon carbide paper, rinsed with ultrapure water (Millipore Milli-Q), immersed for 2 h in a boiling KOH solution, and rinsed again with ultrapure water.

The gold–graphite electrodes were obtained by depositing the metal from a solution of $1 \times 10^{-4} \text{ M Au(III)}$ and 3 M HCl at -430 mV (SCE) for 1 h. The optimum amount of gold was determined as $58 \mu\text{g}/\text{cm}^2$.

A 3 M HCl solution was chosen because it has been demonstrated [9] that high concentrations of this acid favour the reversibility of the Cr(III)/Cr(II) redox couple. For this particular value of the concentration there is a remarkable shifting of the chloro–chromium-complex equilibria to the dichloro-complex species that is a more electroactive species than that of the aquo complex.

All potentials are referred to the saturated calomel electrode (SCE). A carbon felt was used as counter electrode. All the chemical products used, HCl, CrCl_3 , FeCl_2 , PbCl_2 and Bi_2O_3 were Merck p.a. The gold solution was obtained by dissolving pure metal (99.99%) in aqua regia. The solutions were deoxygenated with nitrogen (N-45-SEO) before each experiment.

Redox flow cell characteristics

The cell used was a divided filter-press cell with 117 Nafion membrane as separator. The overall system is formed from the cell, two storage tanks and two magnetic pumps.

Two kinds of electrodes, as described earlier, graphite and gold-graphite both with a geometric area of 60 cm^2 , were used. For both electrolytes,

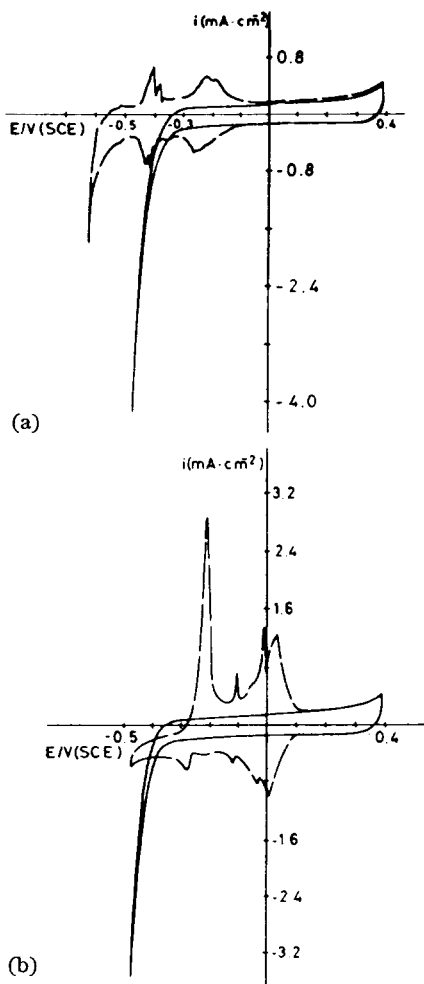


Fig. 1. Comparison of hydrogen evolution on predeposited gold-graphite electrode in 3 M HCl solution (—): (a) 2.2×10^{-3} M Pb(II) ; (b) 5×10^{-3} M Bi(III) ; scan rate 50 mV/s .

posilite and negalite, a 1.25 M $\text{FeCl}_2 + 1.25$ M CrCl_3 in 3 M HCl solution was used. In the negalite, PbCl_2 or BiCl_3 was added. The solutions were deoxygenated by nitrogen bubbling.

Results and discussion

In this study two kinds of gold-graphite electrodes were used. The first one was a gold-graphite electrode on which the different metals, Pb or Bi, were deposited. Gold was previously deposited from a metal chloride solution. The second one was a graphite electrode on which gold and lead or bismuth were codeposited.

Deposits of lead and bismuth on a gold-graphite electrode. Voltammetric behaviour

The effect of different concentrations of lead and bismuth on the hydrogen evolution reaction is shown in Fig. 1. A large shift to more negative potentials of this undesired reaction is observed. The metal concentration that shows the highest inhibiting effect is around 10^{-3} M.

In order to select the most suitable electrocatalytic conditions for a 0.5 M Cr(III) + 3 M HCl solution, the concentration of metallic ion in the solution was varied from 8×10^{-4} M to its optimum value. When the concentration of the metallic ion increases, a separation of the Cr(III)/Cr(II) and hydrogen reaction is clearly observed. A decrease in the peak potential difference

TABLE 1
Optimum concentration values

Electrode	$[\text{M}^{n+}]$ (Molar)	ΔE_p (mV)	R_c ($\Omega \text{ cm}^2$)	R_d ($\Omega \text{ cm}^2$)
(a) Electrolyte 0.5 M CrCl_3 in 3 M HCl				
C	$[\text{Pb}^{2+}] = 6 \times 10^{-4}$	245		
	$[\text{Bi}^{3+}] = 2 \times 10^{-3}$	200		
C-Au	$[\text{Pb}^{2+}] = 2 \times 10^{-3}$	170		
	$[\text{Bi}^{3+}] = 3 \times 10^{-3}$	170		
C	$[\text{Pb}^{2+}] = 8 \times 10^{-4}$ $[\text{Au}^{3+}] = 5 \times 10^{-6}$	190		
	$[\text{Bi}^{3+}] = 2 \times 10^{-3}$ $[\text{Au}^{3+}] = 10^{-5}$	220		
(b) Electrolyte 1.25 M CrCl_3 in 3 M HCl				
C	$[\text{Pb}^{2+}] = 2 \times 10^{-3}$	320	3.45	3.36
	$[\text{Bi}^{3+}] = 1.4 \times 10^{-3}$	290	2.94	2.86
C-Au	$[\text{Pb}^{2+}] = 3 \times 10^{-3}$	300	3.49	3.56
	$[\text{Bi}^{3+}] = 3 \times 10^{-3}$	290	4.63	4.30
C	$[\text{Pb}^{2+}] = 2 \times 10^{-3}$ $[\text{Au}^{3+}] = 5 \times 10^{-6}$	280		
	$[\text{Bi}^{3+}] = 3 \times 10^{-3}$ $[\text{Au}^{3+}] = 10^{-5}$	290		

$\Delta E_p = E_{p,a} - E_{p,c}$) for the Cr(III)/Cr(II) reaction is also observed, which implies an increase in the electrochemical-standard-rate constant of this reaction.

The smallest peak potential differences found were 0.170, and 0.170 V for Pb and Bi, respectively. The concentration values corresponding to these peak differences are given in Table 1(a). Higher concentrations do not seem to modify the redox process behaviour.

For the sake of comparison, when only a graphite electrode is used, the optimum values obtained for ΔE_p are: 0.245 and 0.200 V for Pb and Bi, respectively (Table 1(a)).

The influence of an increase of Cr(III) concentration from 0.5 to 1.25 M (concentration used in the redox cell) on the voltammograms is shown in Fig. 2, and the ΔE_p and catalyst optimum concentration values are presented in Table 1(b).

Therefore, the existence of gold on the electrode produces an increase in the Cr(III)/Cr(II) reversibility especially for a chromium concentration of

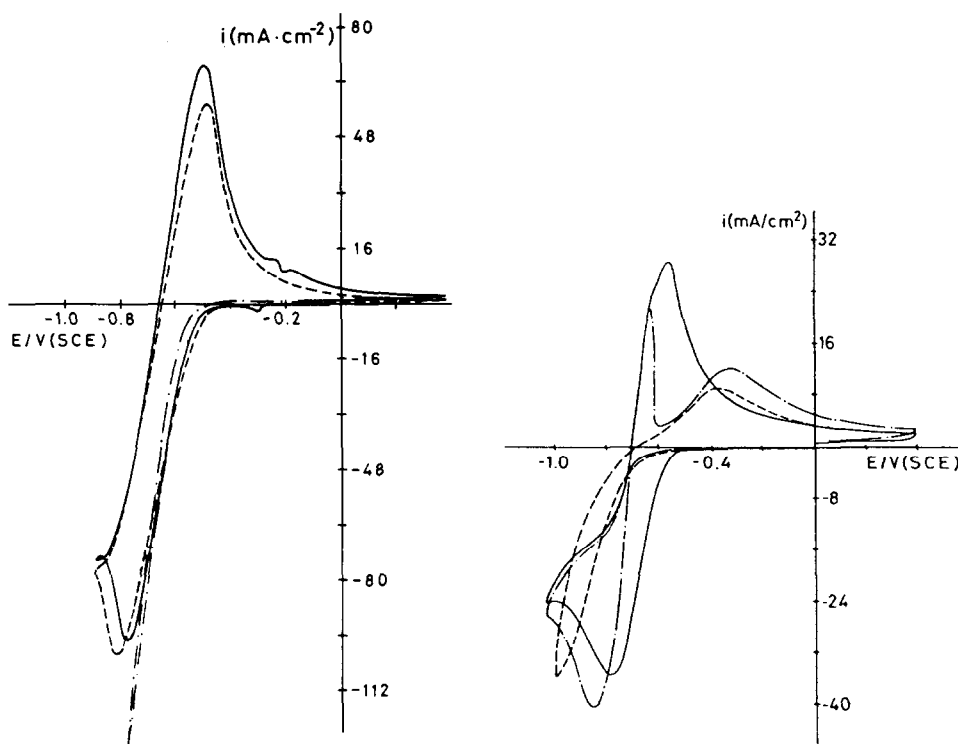


Fig. 2. Cyclic voltammograms of the Cr(III)/Cr(II) system on gold-graphite electrode. Electrolyte: (---) 1.25 M CrCl₃ in 3 M HCl solution; (- - -) with 3×10^{-3} M Pb(II); (—) with 3×10^{-3} M Bi(III); scan rate 50 mV/s.

Fig. 3. Cyclic voltammograms of Cr(III)/Cr(II) system on graphite electrode. Electrolyte: (---) 0.5 M CrCl₃ in 3 M HCl solution; (- - -) 4×10^{-4} M Pb(II) and 10^{-7} M Au(III); (—) 4×10^{-4} M Pb(II) and 10^{-3} M Au(III); scan rate 50 mV/s.

0.5 M. However, for a higher chromium concentration the influence of the presence of gold is less significant.

Voltammetric cycles in the range -380 to -580 mV were made to test the stability of the gold-graphite electrodes. These limit potential values were selected in agreement with the potentials that are attained in the negative electrode of the Fe/Cr redox cell during the charge-discharge process. It was observed that the values of ΔE_p and the anodic-cathodic peak current density are constant through 2000 cycles showing that these electrodes are stable during the potential cycling.

Codeposits of gold and lead or gold and bismuth on graphite electrodes. Voltammetric behaviour

On graphite electrodes, the reduction process of Cr(III) and hydrogen evolution are superimposed and only a small amount of Cr(II) is formed and consequently oxidized during the positive scan. The oxidation process gives a broad peak centered at -0.43 V, Fig. 3.

For a 0.5 M Cr(III) + 3 M HCl solution with a very low gold concentration ($< 10^{-7}$ M) the presence of lead produces a separation between the Cr(III) reduction and the hydrogen evolution, increasing the quantity of Cr(II) formed. During the positive scan two peaks are obtained. The first one corresponds

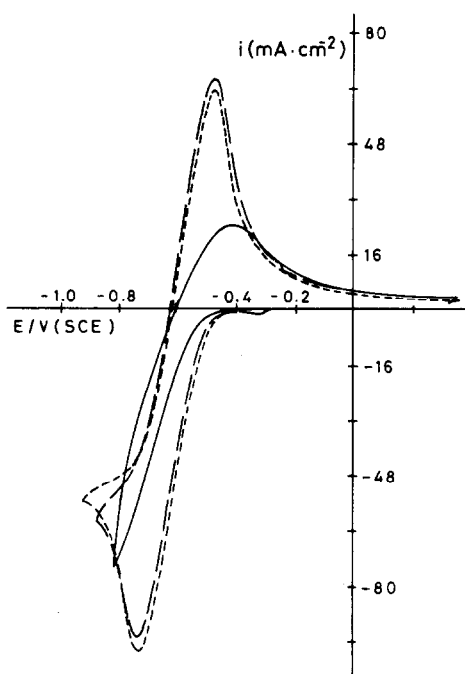


Fig. 4. Cyclic voltammograms of Cr(III)/Cr(II) system on graphite electrode. Electrolyte: (—) 1.25 M CrCl₃ in 3 M HCl solution; (---) 3×10^{-3} M Bi(III) and 10^{-5} M Au(III); (-·-·-) 2×10^{-3} M Pb(II) and 5×10^{-6} M Au(III); scan rate 50 mV/s.

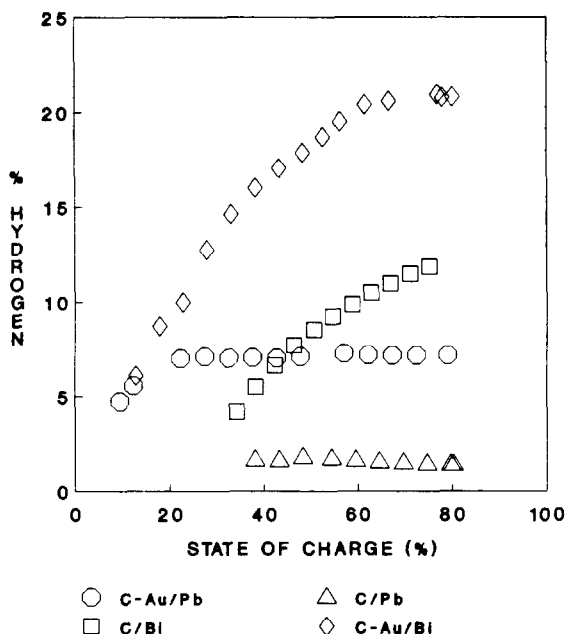


Fig. 5. Percentage of hydrogen formation with respect to the charging state during the first cycle of charge, in mixed electrolytes at 20 mA/cm².

to the dissolution of lead deposit. The second one is placed at the same potentials as that of the peak obtained for the Cr(II) oxidation on graphite. So the presence of very low quantities of gold does not catalyse Cr(II) oxidation.

If the gold concentration is increased at constant lead concentration (4×10^{-4} M), the peak corresponding to Cr(III) reduction is shifted to more positive potentials and the peak corresponding to Cr(II) oxidation is shifted in the opposite direction. So an enhancement of system reversibility is produced. The optimum values obtained for ΔE_p are 0.190 V for $(\text{Au}^{3+}) = 5 \times 10^{-6}$ M and $(\text{Pb}^{2+}) = 8 \times 10^{-4}$ M.

For a 1.25 M Cr(III) + 3 M HCl solution the optimum values obtained for ΔE_p are 0.280 V for $(\text{Au}^{3+}) = 5 \times 10^{-6}$ M and $(\text{Pb}^{2+}) = 2 \times 10^{-3}$ M (Fig. 4).

If gold and bismuth are present in the solution, the optimum value for ΔE_p is 0.290 V for $(\text{Au}^{3+}) = 10^{-5}$ M and $(\text{Bi}^{3+}) = 3 \times 10^{-3}$ M (Fig. 4).

It can be concluded that the presence of gold on the electrode, either predeposited or codeposited, increases the reversibility on the Cr(III)/Cr(II) system especially for low Cr(III) concentration.

Monopolar redox flow cell. Results

A decisive factor for the selection of the most suitable electrode for the Cr(III)/Cr(II) redox system is the amount of hydrogen gas evolved for different states of charge.

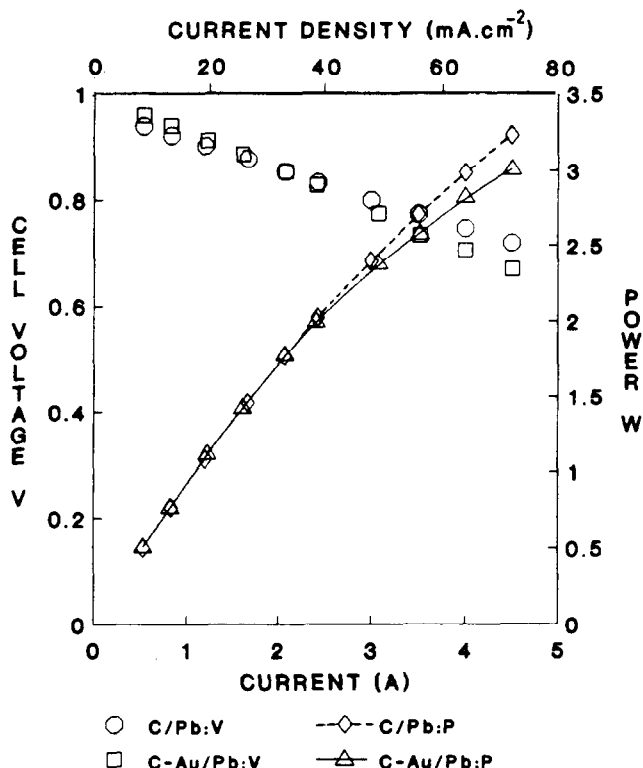


Fig. 6. Current-voltage cell and current-power characteristics of a monopolar redox flow battery at 50% state of discharge.

Figure 5 shows the variation of hydrogen evolution on different electrodes and for different states of charge. For all the electrodes studied, an enhancement of hydrogen evolution is observed with the increase of the state of charge. From this point of view, the best electrode is the C-Pb electrode, though lead is not a good catalyst for the Cr(III)/Cr(II) system especially for the Cr(II) oxidation process.

The C-Au/Pb and C-Au/Bi electrodes behave better electrochemically than the C-Pb and C-Bi electrodes (overtoltage: 15–20 mV for C-Pb or C-Bi to 3–9 mV for C-Au/Pb or C-Au/Bi), though there is an enhancement of hydrogen evolution, especially for the C-Au/Bi electrode.

For all electrodes the variation of the cell voltage versus the current density is lineal until $70 \text{ mA}/\text{cm}^2$, meaning that all the cell voltage drop is resistive under these conditions. In Table 1(b) the values of cell resistivity, both in charge (R_c) and discharge (R_d) modes, for the different electrodes studied, are presented.

Figure 6 shows the variation of cell voltage and power in the discharge mode versus current density.

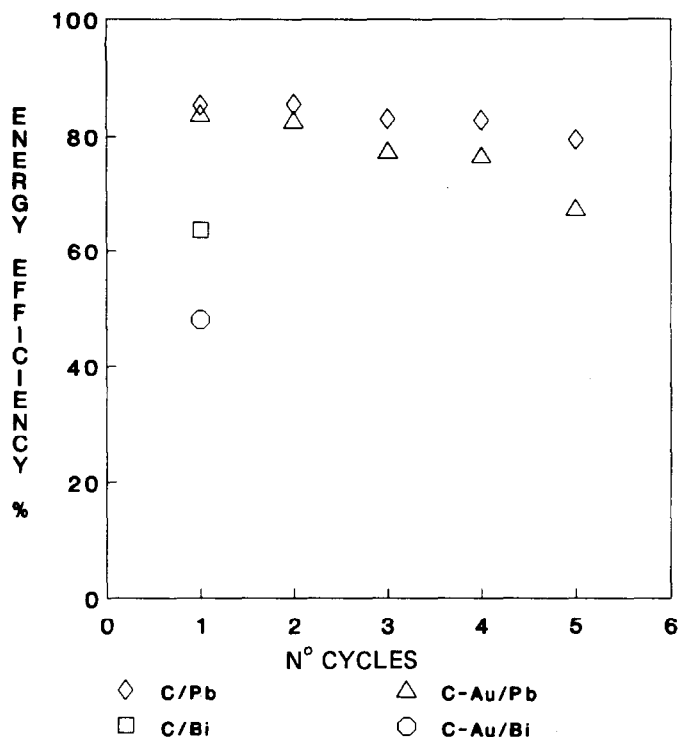


Fig. 7. Variation of the battery efficiency with number of cycles (20 mA/cm² current density).

The energetic efficiency (evaluated between 20 and 80% of state of charge) and its variation with the number of charge–discharge cycles are shown in Fig. 7 for a density current of 20 mA/cm². The better behaviour of the C–Pb electrode against the C–Au/Pb electrode is due to its higher hydrogen overvoltage, though the presence of gold on the electrode diminished the Cr(III)/Cr(II) overvoltage by 80%.

Due to the great amount of hydrogen formed on the C–Au/Bi electrode, especially at high states of charge, it has been impossible to study the variation of the energetic efficiency with the number of charge–discharge cycles without rebalancing the electrolytes after each charge–discharge cycle. If the results of the first cycle are compared for all the electrodes used, it may be found that the energetic efficiency of the C–Au/Bi electrode is very low compared with the energetic efficiency obtained for the C–Au/Pb electrode.

Conclusions

The behaviour of the redox reactions Cr(III)/Cr(II) and hydrogen evolution on gold–graphite surfaces has been studied. Different metals with high hydrogen overvoltage have been used. An enhancement in the reversibility

of the redox couple is obtained with gold-graphite electrodes. This enhancement of the Cr(III)/Cr(II) system reversibility does not provide a parallel increase in the energetic efficiency of the cell for the C-Au/Pb and C-Au/Bi electrodes due to the greater evolution of hydrogen.

It can therefore be concluded that the use of gold as an electrocatalyst of the Cr(III)/Cr(II) system in an Fe/Cr redox cell is not necessary for the acceptable behaviour of the cell.

Acknowledgements

This project was supported by Hidroelectrica Española S.A. The collaboration of J. Medina and M. A. Pastor is also acknowledged.

Reference

- 1 L. H. Thaller, in *Proc. 9th Inter-Society Energy Conversion Engineering Conf., San Francisco, CA, Aug. 26-30, 1974*, American Society of Mechanical Engineers, p. 924 (NASA TMX-71540).
- 2 J. Giner, L. Swette and K. Cahill, *NASA CR-134705*, 1976.
- 3 E. Sum and M. Skyllas-Kazacos, *J. Power Sources*, **15** (1985) 179-190.
- 4 L. H. Thaller, Dept. of Energy, DC, *DOE/NASA 1002-79/4*, Washington, DC, *NASA TM-79186*, 1979.
- 5 L. H. Thaller, Dept. of Energy, DC, *DOE/NASA/1002-79/3*, Washington, DC, *NASA TM-79143*, 1979.
- 6 Moonlight Project: Advanced Battery Electric Energy Storage System, *NEDO, 10*, Japan, 1988.
- 7 H. Knobloch, W. Kellermann, H. Nischik, K. Pantel and G. Siemsen, *Siemens Forsch., U. Entwickl. Ber.*, **12** (1983) 2, 79.
- 8 P. Garces, M. A. Climent and A. Aldaz, *An. Quím.*, **83** (1987).
- 9 M. A. Climent, P. Garces, M. Lopez-Segura and A. Aldaz, *An. Quím.*, **83** (1987) 12.
- 10 J. Giner and K. J. Cahill, *NASA Tech. Rep. CR-159738*, 1979.
- 11 C. Y. Yang, *J. Appl. Electrochem.*, **12** (1982) 425.
- 12 C. D. Wu, D. A. Scherson, E. J. Calvo and E. B. Yeager, *J. Electrochem. Soc.*, **133** (1986) 2109.
- 13 D. Sh. Cheng and E. Hollax, *J. Electrochem. Soc.*, **132** (1985) 269.
- 14 V. Jalan, M. Stark and J. Giner, NASA-Lewis Research Center, Contract DEN 3-97, *CR-165218*, 1981.